

## OPEN ACCESS

## EDITED BY

Jose Federico Carrillo,  
National Institute of Cancerology (INCAN),  
Mexico

## REVIEWED BY

Renfei Wang,  
Shanghai Jiao Tong University Affiliated  
Sixth People's Hospital, China  
Chentian Shen,  
Shanghai Sixth People's Hospital, China

## \*CORRESPONDENCE

Jun Liang

✉ liangjun1959@aliyun.com

Yansong Lin

✉ linsy@pumch.cn

†These authors have contributed  
equally to this work and share  
first authorship

## SPECIALTY SECTION

This article was submitted to  
Thyroid Endocrinology,  
a section of the journal  
Frontiers in Endocrinology

RECEIVED 27 November 2022

ACCEPTED 27 January 2023

PUBLISHED 10 February 2023

## CITATION

Meng C, Song J, Long W, Mu Z, Sun Y,  
Liang J and Lin Y (2023) A user-friendly  
nomogram for predicting radioiodine  
refractory differentiated thyroid cancer.  
*Front. Endocrinol.* 14:1109439.  
doi: 10.3389/fendo.2023.1109439

## COPYRIGHT

© 2023 Meng, Song, Long, Mu, Sun, Liang  
and Lin. This is an open-access article  
distributed under the terms of the [Creative  
Commons Attribution License \(CC BY\)](#). The  
use, distribution or reproduction in other  
forums is permitted, provided the original  
author(s) and the copyright owner(s) are  
credited and that the original publication in  
this journal is cited, in accordance with  
accepted academic practice. No use,  
distribution or reproduction is permitted  
which does not comply with these terms.

# A user-friendly nomogram for predicting radioiodine refractory differentiated thyroid cancer

Chao Meng<sup>1,2,3,4†</sup>, Juanjuan Song<sup>5†</sup>, Wen Long<sup>6</sup>,  
Zhuanzhuan Mu<sup>2,3</sup>, Yuqing Sun<sup>2,3</sup>, Jun Liang<sup>1,4\*\*</sup>  
and Yansong Lin<sup>2,3\*</sup>

<sup>1</sup>Department of Oncology, Key Laboratory of Carcinogenesis and Translational Research (Ministry of Education/Beijing), Peking University Cancer Hospital & Institute, Beijing, China, <sup>2</sup>Department of Nuclear Medicine, State Key Laboratory of Complex Severe and Rare Diseases, Peking Union Medical College (PUMC) Hospital, Chinese Academy of Medical Sciences & PUMC, Beijing, China, <sup>3</sup>Beijing Key Laboratory of Molecular Targeted Diagnosis and Therapy in Nuclear Medicine, Beijing, China, <sup>4</sup>Department of Oncology, Peking University International Hospital, Beijing, China, <sup>5</sup>Department of Nuclear Medicine, Peking University International Hospital, Beijing, China, <sup>6</sup>Department of Nuclear Medicine, State Key Laboratory of Oncology in South China, Sun Yat-sen University Cancer Center, Guangzhou, China

**Background:** The diagnosis of radioiodine refractory differentiated thyroid cancer (RAIR-DTC) is primarily based on clinical evolution and iodine uptake over the lesions, which is still time-consuming, thus urging a predictive model for timely RAIR-DTC informing. The aim of this study was to develop a nomogram model for RAIR prediction among DTC patients with distant metastases (DM).

**Methods:** Data were extracted from the treatment and follow-up databases of Peking Union Medical College Hospital between 2010 and 2021. A total of 124 patients were included and divided into RAIR (n=71) and non-RAIR (n=53) according to 2015 ATA guidelines. All patients underwent total thyroidectomy followed by at least two courses of RAI treatment. Serological markers and various clinical, pathological, genetic status, and imaging factors were integrated into this study. The pre-treatment stimulated Tg and pre- and post-treatment suppressed Tg at the first and second course RAI treatment were defined as s-Tg1, s-Tg2, sup-Tg1, and sup-Tg2, respectively.  $\Delta$ s-Tg denoted s-Tg1/s-Tg2, and  $\Delta$ s-TSH denoted s-TSH1/s-TSH2. Multivariate logistic regression and correlation analysis were utilized to determine the independent predictors of RAIR. The performance of the nomogram was assessed by internal validation and receiver operating characteristic (ROC) curve, and benefit in clinical decision-making was assessed using decision curve.

**Results:** In univariate logistic regression, nine possible risk factors were related to RAIR. Correlation analysis showed four of the above factors associated with RAIR. Through multivariate logistic regression,  $\Delta$ s-Tg/ $\Delta$ s-TSH<1.50 and age upon diagnosis were obtained to develop a convenient nomogram model for predicting RAIR. The model was internally validated and had good predictive efficacy with an AUC of 0.830, specificity of 0.830, and sensitivity of 0.755. The decision curve also showed that if the model is used for clinical decision-making when the probability threshold is between 0.23 and 0.97, the net benefit of patients is markedly higher than that of the TreatAll and TreatNone control groups. By using

1.50 as a cut-off of  $\Delta s\text{-Tg}/\Delta s\text{-TSH}$ , differing biochemical progression among the generally so-called RAIR can be further stratified as meaningfully rapidly or slowly progressive patients ( $P=0.012$ ).

**Conclusions:** A convenient user-friendly nomogram model was developed with good predictive efficacy for RAIR. The progression of RAIR can be further stratified as rapidly or slowly progressive by using 1.50 as a cut-off value of  $\Delta s\text{-Tg}/\Delta s\text{-TSH}$ .

#### KEYWORDS

neoplasm metastasis, thyroid cancer, thyroglobulin, radioiodine refractory, nomogram

## Introduction

The incidence of thyroid cancer has kept rising globally (1). Differentiated thyroid cancer (DTC) accounts for more than 90% of thyroid cancers and consists mainly of papillary thyroid cancer (PTC) and follicular thyroid cancer (FTC) (2, 3). Most DTCs carry a favorable prognosis after thyroidectomy, selective radioactive iodine (RAI) treatment, and thyroid stimulating hormone (TSH) -suppressive treatment. However, roughly 7-23% of DTC patients develop distant metastases (DM) (4-6). Among these patients, two-thirds become radioiodine refractory DTC (RAIR-DTC) and have a much lower 10-year survival rate than those RAI responsive patients (10 vs. 56%), which is the most common cause of cancer-related deaths, and pose a great challenge in the management of DTC (7-9). Given the lack of benefit of repeated RAI treatment to these patients and the increasing risk of side effects, timely identifying the RAIR-DTC is imperative for such patients to avoid unnecessary RAI treatment and gain more time for the effective treatment regimen like Multi-Kinase Inhibitors (MKIs).

The definition of RAIR has been outlined in the 2015 ATA guidelines (10), which are mainly based on imaging manifestation characterized by the loss of radioiodine uptake and increasing level of the tumor marker thyroglobulin (Tg). Of note, the diagnosis of RAIR-DTC is primarily based on clinical evolution and iodine uptake characteristics rather than pathological characteristics. While controversies existed particularly in terms of the predictive value of  $^{131}\text{I}$  whole body scan ( $^{131}\text{I}$ -WBS) imaging and imaging heterogeneity among multiple metastases (11). Thus the ultimate identification still requires long-term follow-up after RAI treatment, which is time-consuming and often induces a delayed judgment that deprives access to timely and effective therapeutic approaches.

Over recent years, clinicopathological characteristics, as well as molecular features, have been recognized as meaningful indicators that could be utilized for RAIR prediction. And factors like older age, larger primary tumor size, extrathyroidal extension (ETE), BRAF<sup>V600E</sup> mutation, TERT promoter mutation, and high-risk histological subtypes were reported to be correlated with RAIR-DTC respectively, according to different retrospective studies, with an unfavorable median overall survival (OS) (12-14). While factors identified in each study alone still showed poor performance in predicting individual risk of RAIR, thus a predictive model is needed to integrate multiple factors as a whole. The nomogram is an effective model that takes the weights of relevant factors into consideration and integrates the independent

factors for predicting the risk probability of a special clinical event, which is valuable for clinical decision-making and risk stratification (15, 16). Only two studies have reported the nomogram model to predict RAIR-DTC so far to our knowledge, which mainly took static clinicopathologic and costly  $^{18}\text{F}$ -FDG PET/CT molecular imaging features into account, while both of which lacked dynamic assessment and were not universally available due to economic burden (17, 18). While Tg as the most critical real-time tumor marker was ignored, which has an irreplaceable role in the follow-up and management of thyroid cancer after surgery to predict recurrence and metastasis and assess long-term survival (19-22).

This study aims to develop a prediction nomogram model of RAIR by integrating serological markers such as Tg, various clinical, pathological, genetic status, and imaging factors for predicting RAIR among patients with DM-DTC.

## Patients and methods

The study protocol was approved by the ethical board of the Chinese Academy of Medical Sciences and Peking Union Medical College Hospital (PUMCH).

### Patients

In this retrospective study, we extracted data for all DM-DTC patients ( $n=369$ ) from 2205 thyroid cancer patients treated with total or near-total thyroidectomy followed by RAI treatment between 2010 and 2021, with follow-up through November 1, 2021. Patients with DM-DTC were defined with any of the following: ① metastatic lesions confirmed by pathology, ② focal or diffuse uptake in metastatic lesions on  $^{131}\text{I}$ -WBS after excluding the contamination and physiological RAI uptake, with or without positive findings on other complementary imaging modalities (chest CT, x-rays, MRI, bone scintigraphy or  $^{18}\text{F}$ -FDG PET/CT) or elevated Tg levels, ③ positive findings on  $^{18}\text{F}$ -FDG PET/CT after excluding other malignancies and benign diseases, with a rising Tg level, despite of the negative  $^{131}\text{I}$ -WBS results, ④ negative findings on functional imaging, but structural lesions suggested by other imaging instruments with a rising Tg level after excluding other malignancies and benign diseases. Patients' exclusion criteria with either of the following: ① no distant metastatic lesions identified on

imaging, ② absence of serial serological data, ③ absence of information on the first two rounds of RAI treatment, ④ absence of follow-up information.

RAIR definition was based on the 2015 ATA guidelines: (i) the malignant/metastatic tissue does not ever concentrate RAI (no uptake outside the thyroid bed at the first therapeutic WBS), (ii) the tumor tissue loses the ability to concentrate RAI after previous evidence of RAI-avid disease (in the absence of stable iodine contamination), (iii) RAI is concentrated in some lesions but not in others; and (iv) metastatic disease progresses despite significant concentration of RAI (10). A total of 124 DM-DTC patients were finally enrolled (Figure 1). The overall median follow-up was 51.5 months (interquartile range:32.75,70.00 months). Patients were further divided into non-RAIR and RAIR.

## Postoperative RAI treatment

A serum thyroid stimulating hormone (TSH) level higher than 30mU/L was achieved by thyroid hormone withdrawal (THW) before RAI treatment. All patients were instructed with a low iodine diet from the beginning of THW to 3 weeks after RAI treatment. Patients were administered with a range of 3.7–7.4GBq (100–200mCi) RAI treatment dose. Repeated RAI treatment was usually performed 6 to 12 months after the previous treatment.

Stimulated or suppressed Tg (s-Tg or sup-Tg), TSH, and thyroglobulin antibody (TgAb) were usually tested 1 day before and 2–3 months after RAI treatment. S-Tg was defined as Tg measured after THW with a TSH level >30 mU/L. The s-Tg and TSH on the day of the first (s-Tg1, s-TSH1) and second (s-Tg2, s-TSH2) course of RAI

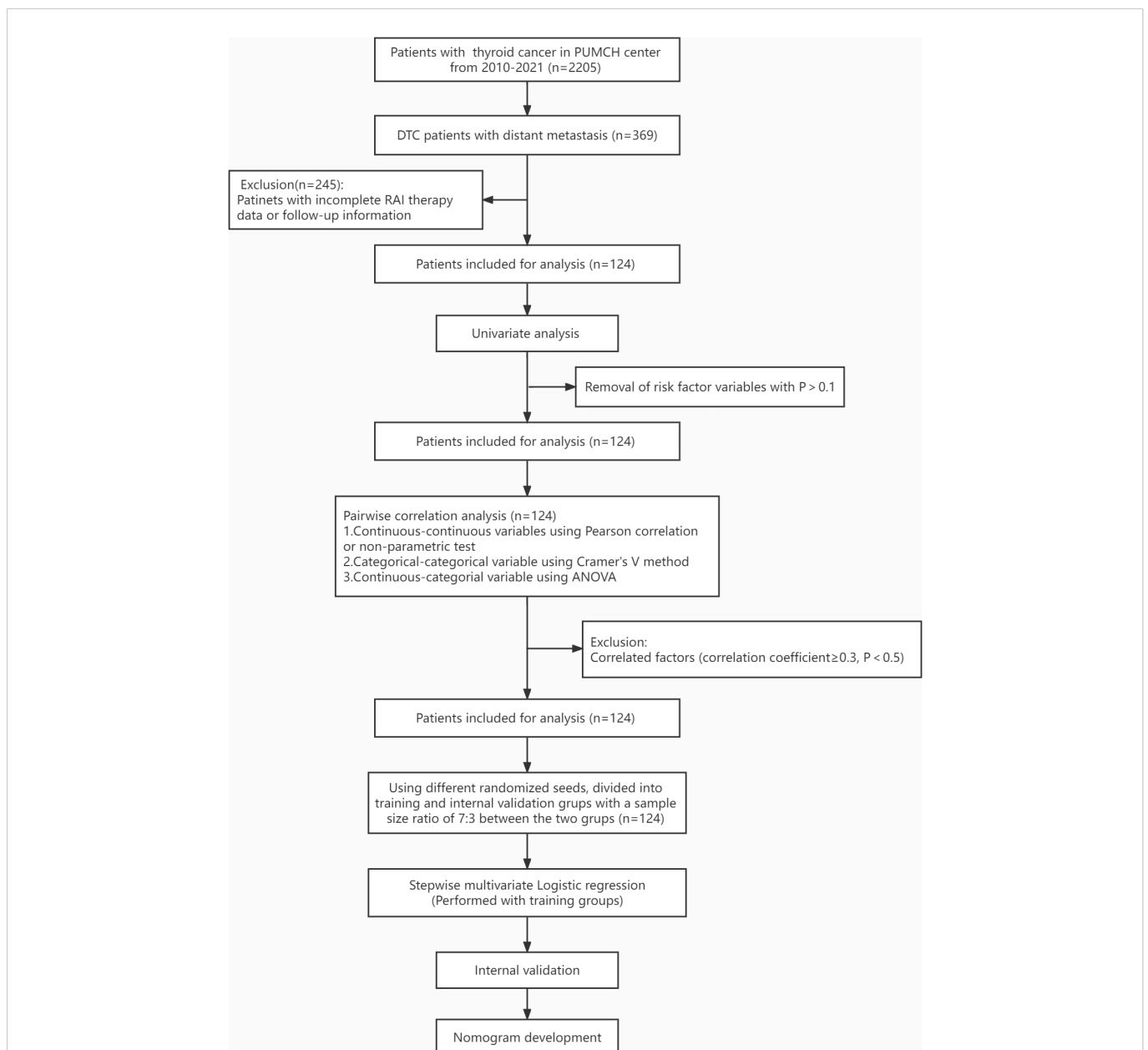


FIGURE 1

Workflow for patient selection and development of the nomogram model to predict RAIR among DM-DTC patients. PUMCH, Peking Union Medical College Hospital; RAIR, radioiodine refractory; DM, distant metastases; DTC, differentiated thyroid cancer.

treatment and the suppressed Tg at 1 to 3 months before (sup-Tg1) and 3 months after (sup-Tg2) the second RAI treatment were further analyzed to detect the prediction value. Post-therapeutic whole-body scan (Rx-WBS) was performed 5–7 days after RAI treatment. CT without contrast was carried out as needed. All patients were under TSH suppressive treatment using sodium levothyroxine to achieve a TSH level  $<0.1\mu\text{IU/mL}$  during courses of RAI treatment and subsequent follow-up.

## Measurement of Tg, TgAb and TSH

Tg and TgAb levels were determined by electrochemiluminescence immunoassay (Roche Diagnostics GmbH, Mannheim, Germany) with a functional sensitivity of  $0.100\text{ ng/mL}$  and  $10\text{ IU/mL}$ , respectively. TSH was determined by chemiluminescence immunoassay (Siemens Healthcare Diagnostics Inc, New York, New York, USA), with a measuring range from  $0.004$  to  $150\mu\text{IU/mL}$ . TgAb values  $>115\text{ IU/mL}$  were considered positive. Rx-WBS was obtained in the anterior and posterior projections using dual-head gamma cameras (Infinia Hawkeye; GE, Fairfield, Connecticut, USA) equipped with high-energy parallel-hole collimators, and a 20% energy window was centered at  $364\text{ keV}$ , at a table speed of  $20\text{ cm/min}$  for a total time of  $15\text{ min}$  ( $256\times 1024$  matrix).

## Biochemical progression

The sup-Tg level in all samples with TSH level  $<0.1\mu\text{IU/mL}$  and TgAb negativity ( $\leq 115\text{ IU/mL}$ ) was examined. Biochemical progression was defined as  $>20\%$  increase in sup-Tg level at follow-up compared with that after thyroid remnant ablation (23).

## Gene analysis

Genomic DNA was extracted from either primary or lymph-node metastatic DTC tumors, which were sliced into  $5\mu\text{m}$ -thick sections, fixed with formalin and embedded in paraffin. BRAF and TERT mutations were analyzed by real-time fluorescent quantitative polymerase chain reaction (PCR). Exon 15 of the BRAF gene containing the site for the T1799A (V600E) mutation was amplified using primers 5'-TGCTTGCTCTGATAGGAAAA TG-3'(sense) and 5'-AGCCTCAA TTCTTACCA TCCA-3'(antisense). The TERT promoter includes two mutation hotspots: C228T and C250T. A 193-bp fragment of the TERT promoter was amplified by PCR using approximately  $100\text{ ng}$  of genomic DNA and primers 5'-CACCCGTCTGCCCCCTCACCTT-3'(sense) and 5'-GGCTTCCCACGTGCGCAGCAGGA-3'(antisense). The real-time fluorescent quantitative PCR protocol comprised an initial denaturation for  $5\text{ min}$  at  $95^\circ\text{C}$ , 15 cycles of template enrichment (denaturation for  $25\text{ s}$  at  $95^\circ\text{C}$ , annealing for  $20\text{ s}$  at  $64^\circ\text{C}$ , and extension for  $20\text{ s}$  at  $72^\circ\text{C}$ ), and 31 amplification cycles (denaturation for  $25\text{ s}$  at  $93^\circ\text{C}$ , annealing for  $35\text{ s}$  at  $60^\circ\text{C}$ , and amplification cycles (denaturation for  $25\text{ s}$  at  $93^\circ\text{C}$ , annealing for  $35\text{ s}$  at  $60^\circ\text{C}$ , and DNA Analyzer.

## Data processing and statistical analysis

All factors included in the analysis were divided into categorical and continuous variables, with no special processing for the former.

Continuous variable were handled as follows: ① remove outliers: Data less than the 1st quartile minus 1.5 times the quartile difference were replaced with the 5% quantile and data greater than the 3rd quartile plus 1.5 times the quartile difference were replaced with the 95% quantile; ② remove the Tg for TgAb  $>115\text{ IU/mL}$ ; ③ ROC curves were plotted for each continuous variable against the RAIR status, and variables with AUC value  $>0.7$  were then transformed to corresponding categorical variables. A dataset was then derived after removing highly subjective variables such as TSH levels, cumulative dose, and cumulative number of RAI treatment. Very incomplete variables were removed to get the final dataset. Univariate and multivariate logistic regression was then applied to this dataset. Figure 1 shows the workflow chart for patient selection and model construction.

Statistical analysis was performed using the R software (version 4.1.2). The packages in R that were used in this study are reported in the Data Supplementary. The reported statistical significance levels between groups were all two-sided, with statistical significance set at 0.05.

The Kaplan-Meier and log-rank analyses were used to assess Tg progression-free survival (Tg-PFS).

## Results

### Clinicopathologic characteristics of patients

Of 124 patients included in the analysis, 118 (95.2%) had PTC, 5 (4.0%) had FTC and 1 (0.8%) had PTC combined with FTC. The baseline clinicopathologic characteristics of 124 DM-DTC patients, including 42 men and 82 women, with a male/female ratio of 1:1.95, are summarized in Table 1. With the criteria for judgment, 71 patients were identified as RAIR, 53 as non-RAIR, and one RAIR case fulfilled criteria ii and iii. Patients with RAIR were more likely to be older upon diagnosis and with more advanced T staging ( $P=0.021$  and  $0.015$ , respectively). RAIR tended to have higher capsular invasion rate and larger tumor size ( $P=0.059$  and  $0.147$ , respectively). There were no statistical differences in terms of gender, tumor lesion, multifocality, and N staging.

### Serological characteristics in RAIR and non-RAIR patients

Serological follow-up was performed on 124 patients with DM-DTC before and after the first and second RAI treatment (Table 1). TSH, Tg and TgAb results did not differ between the two groups before and after the first RAI treatment. Both s-Tg2 and sup-Tg2 were significantly higher in RAIR group ( $P=0.02$ , and  $0.027$ , respectively). Additionally,  $\Delta\text{s-Tg}$  (s-Tg1/s-Tg2) was remarkably lower in RAIR than the in non-RAIR group ( $P<0.001$ ). To minimize the influence of TSH,  $\Delta\text{s-Tg}/\Delta\text{s-TSH}$  (s-TSH1/s-TSH2) was also calculated in the analyses.  $\Delta\text{s-Tg}/\Delta\text{s-TSH}$  in RAIR was significantly lower compared to non-RAIR ( $P<0.001$ ) and was also more evident than that of  $\Delta\text{s-Tg}$ . A cut-off value of  $\Delta\text{s-Tg}/\Delta\text{s-TSH}$  at 1.50 was obtained with a sensitivity of 0.831, specificity of 0.792, and AUC of 0.818, respectively (Figure 2).

TABLE 1 Clinicopathologic Characteristics of 124 Patients with DM-DTC.

Characteristics	Total (N=124)	Non-RAIR (N=53)	RAIR (N=71)	P
Age upon diagnosis (year) [mean (SD)]	35.10 (15.60)	31.38 (12.59)	37.89 (17.08)	0.021
Gender [n (%)]				0.578
Mela	42 (33.90)	16 (30.20)	26 (36.6)	
Female	82 (66.10)	37 (69.80)	45 (63.40)	
Tumor largest dimension (cm) [mean (SD)]	2.58 (1.72)	2.31 (1.59)	2.80 (1.80)	0.147
Cervical lymph node dissection [n (%)]				0.418
Yes	117 (94.40)	52 (98.10)	65 (91.50)	
No	7 (5.60)	1 (1.90)	6 (8.50)	
Pathological subtype [n (%)]				0.098
Classic PTC	29 (23.40)	15 (28.30)	14 (19.70)	
Follicular-variant PTC	36 (29.00)	19 (35.80)	17 (23.90)	
Other subtypes	21 (16.90)	6 (11.30)	15 (21.10)	
Unavailable	38 (30.60)	13 (24.50)	25 (35.20)	
Tumor lesion [n (%)]				0.441
Unilateral	59 (47.60)	28 (52.80)	31 (43.70)	
Bilateral	64 (51.60)	25 (47.20)	39 (54.90)	
Unavailable	1 (0.80)	0 (0.00)	1 (1.40)	
Multifocality [n (%)]				0.351
One lesion	36 (29.00)	19 (35.80)	17 (23.90)	
More than one lesion	80 (64.50)	31 (58.50)	49 (69.00)	
Unavailable	8 (6.50)	3 (5.70)	5 (7.00)	
Capsular invasion [n (%)]				0.059
Yes	102 (82.30)	40 (75.50)	62 (87.30)	
No	12 (9.70)	9 (17.00)	3 (4.20)	
Unavailable	10 (8.10)	4 (7.50)	6 (8.50)	
BRAF <sup>V600E</sup> mutation [n (%)]				0.085
Yes	44 (35.50)	14 (26.40)	30 (42.30)	
No	63 (50.80)	33 (62.30)	30 (42.30)	
Unavailable	17 (13.70)	6 (11.30)	11 (15.50)	
TERT mutation [n (%)]				0.04
Yes	12 (9.70)	1 (1.90)	11 (15.50)	
No	46 (37.10)	21 (39.60)	25 (35.20)	
Unavailable	66 (53.20)	31 (58.50)	35 (49.30)	
AJCC-T Stage [n (%)]				0.015
T1	31 (25.0)	21 (39.6)	10 (14.10)	
T2	12 (9.7)	4 (7.5)	8 (11.30)	
T3	17 (13.7)	4 (7.5)	13 (18.30)	
T4	55 (44.4)	21 (39.6)	34 (47.90)	
Unavailable	9 (7.3)	3 (5.7)	6 (8.50)	

(Continued)

TABLE 1 Continued

Characteristics	Total (N=124)	Non-RAIR (N=53)	RAIR (N=71)	P
AJCC-N Stage [n (%)]				0.235
N0	3 (2.40)	1 (1.90)	2 (2.80)	
N1a	12 (9.70)	6 (11.30)	6 (8.50)	
N1b	100 (80.60)	45 (84.90)	55 (77.50)	
Unavailable	9 (7.30)	1 (1.90)	8 (11.30)	
Serological characteristics (ng/mL) [median (IQR)]				
s-Tg1	344.10 (62.74,500.0)	361.40 (93.14,500.0)	342.20 (60.34-500.0)	0.636
sup-Tg1	14.31 (4.75,77.51)	12.73 (2.76-69.0)	16.30 (5.03-80.04)	0.573
s-Tg2	189.96 (57.23, 500.6)	119.8 (38.44, 466)	250.2 (78.89, 603.6)	0.02
sup-Tg2	11.10 (3.15, 70.44)	7.73 (2.0, 42.37)	16.94 (6.2, 87.49)	0.027
$\Delta$ s-Tg [median (IQR)]	1.06 (0.92, 1.71)	1.69 (1.00,3.7)	1.00 (0.75,1.27)	<0.001
$\Delta$ s-Tg/ $\Delta$ s-TSH [median (IQR)]	1.37 (0.95, 2.68)	2.42 (1.58-4.11)	1.05 (0.79-1.4)	<0.001
$\Delta$ s-Tg/ $\Delta$ s-TSH<1.50 [n (%)]				<0.001
Yes	69 (55.6)	11 (20.8)	58 (81.7)	
No	55 (44.4)	42 (79.2)	13 (18.3)	
Cumulative RAI dose (mCi) [median (IQR)]	340 (300, 450)	450.00 (300, 540)	300.00 (300, 450)	0.05
Number of RAI treatment [n (%)]				0.263
2	63 (50.8)	22 (41.5)	41 (57.7)	
3	35 (28.2)	16 (30.2)	19 (26.8)	
4	12 (9.7)	9 (17.0)	3 (4.2)	
>4	14 (11.3)	6 (11.3)	8 (11.3)	
RAIR according to 2015 ATA guidelines [n (%)]				
i			36 (50.7)	
ii			5 (7.04)	
iii			15 (21.13)	
iv			16 (22.54)	

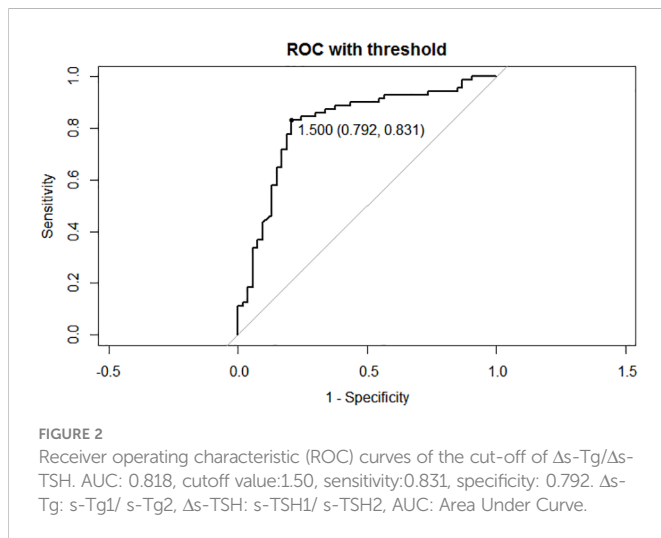
DM, distant metastases; DTC, differentiated thyroid cancer; RAI, radioactive iodine;  $\Delta$ s-Tg, s-Tg1/s-Tg2;  $\Delta$ s-TSH, s-TSH1/ s-TSH2.

## Results of univariate logistic regression and correlation analysis

Univariate logistic regression demonstrated that sup-TgAb1, s-Tg2, sup-Tg2,  $\Delta$ s-Tg,  $\Delta$ s-Tg/ $\Delta$ s-TSH,  $\Delta$ s-Tg/ $\Delta$ s-TSH<1.50, age upon diagnosis, BRAF<sup>V600E</sup> mutation, and AJCC-T stage were opted risk factors for RAIR ( $P<0.1$ , Table 2), among which sup-TgAb1, sup-Tg2, BRAF<sup>V600E</sup> mutation, and AJCC-T stage were removed from dataset due to data incompleteness. The remaining possible risk factors were included into the correlation analysis. Risk factors with a correlation coefficient greater than 0.3 were considered to be correlated factors. In correlation analysis,  $\Delta$ s-Tg was removed because of correlation with both s-Tg2 (correlation factor=-0.323) and  $\Delta$ s-Tg/ $\Delta$ s-TSH (correlation factor=0.743), leaving the following four factors to be opt-independent risk factors: s-Tg2,  $\Delta$ s-Tg/ $\Delta$ s-TSH,  $\Delta$ s-Tg/ $\Delta$ s-TSH<1.50, and age upon diagnosis.

## Multivariate analysis, internal validation, and logistic model construction

Totally, 70% of cases were randomly selected as the training set, and then stepwise multivariate logistic regression was performed using the MASS package (7.3-54) of R. The left 30% of cases were selected as the validation set. Two independent risk factors,  $\Delta$ s-Tg/ $\Delta$ s-TSH<1.50 and age upon diagnosis, were eventually screened for predicting RAIR. The above procedure was performed five times with different randomization seeds, and the results were reliable (Figure 3, Table 3). We then used the two factors ( $\Delta$ s-Tg/ $\Delta$ s-TSH<1.50 and age upon diagnosis) as independent risk factors to generate a linear Logistic regression model to predict RAIR. Based on the two independent factors obtained in stepwise multiple Logistic regression analysis, a nomogram characterized by scale line and score weight reflected to RAIR-DTC prediction was established in



Figures 4A, B; the AUC of the model is 0.830, with a specificity of 0.830 and sensitivity of 0.755. The calibration and decision curves for our final model are also shown in Figures 4C, D, with the p-value for the Hosmer-Lemeshow test for the former being greater than 0.05, indicating our model's probability of predicting RAIR is not significantly different from the actual RAIR situation. The latter shows that our model outperforms the two control groups of TreatAll and TreatNone in terms of the net benefit to patients' clinical decision-making over a relatively significant threshold probability range of 0.24-0.97.

## Impact of $\Delta s\text{-Tg}/\Delta s\text{-TSH}$ cut-off value of 1.50 on Tg-PFS in RAIR patients

The results of the Kaplan-Meier and log-rank analyses of Tg-PFS in patients with RAIR are provided below. The median Tg-PFS (mTg-PFS) in 124 patients was 37 months (95% CI: 37.83-48.82 months). The mTg-PFS was 24.4 months (95% CI: 25.93-38.23 months) and 56 months (95% CI:49.91-66.88months) for RAIR and non-RAIR patients, respectively. An obviously shorter Tg-PFS was observed in RAIR than in non-RAIR ( $\chi^2 = 43.345$ ,  $P=0.000$ ) (Figure 5A).

In the RAIR group, the mTg-PFS was 20.49 months (95% CI: 21.89-33.71 months) for 58 patients with  $\Delta s\text{-Tg}/\Delta s\text{-TSH}<1.50$  and 43.00 months (95% CI:31.58-70.76 months) for 13 patients with  $\Delta s\text{-Tg}/\Delta s\text{-TSH}\geq 1.50$ . The log-rank test showed a significantly shorter Tg-PFS in the former patients compared to the latter ( $\chi^2 = 6.316$ ,  $P = 0.012$ ) (Figure 5B).

## Discussion

In the present study, we retrospectively developed and validated a nomogram model for predicting RAIR in patients with DM-DTC by integrating serological markers and various clinical, pathological, genetic status, and imaging factors. Based on univariate logistic regression, nine possible risk factors were significantly related to RAIR. And correlation analysis showed that four of the above factors displayed associations with RAIR. Two independent predictors of RAIR were finally confirmed in multivariate logistic regression analysis:  $\Delta s\text{-Tg}/\Delta s\text{-TSH}$  and age upon diagnosis, with the former parameter derived from Tg, which would be a dichotomous variable reflecting the dynamic s-Tg changing rate with the cut-off of 1.50. Internal validation was used to determine that the model had good predictive power to predict RAIR. The decision curve with net benefits was further used to assess the model's better clinical predictive value.

Tg has been reported to be a specific biomarker produced by thyroid tissue and DTC lesions, which is well acknowledged as convenient, reproducible, and sensitive to be monitored, particularly after remnant thyroid ablation (10). It plays an essential role in the surveillance of thyroid cancer after surgery to reveal recurrence, metastasis and assess long-term survival (24). Previous researches from our team have shown that qualitative assessment of the Tg levels can help to grade the risk of recurrence and predict metastasis and RAIR in DTC patients with pulmonary metastases (20, 25). The change of Tg during TSH stimulation, such as  $\Delta Tg/\Delta TSH$ , can be used as a specific early biochemical marker for DM-DTC (22). Wang C et al. further analyzed the percentage change of Tg before and after RAI treatment, namely  $\Delta Tg$ , during the first two courses in DM-DTC patients receiving multiple RAIs and showed that it was informative for RAIR (25). Based upon the above findings,  $\Delta s\text{-Tg}/$

TABLE 2 Results of univariate logistic regression.

Characteristics	P	Characteristics	P
Age upon diagnosis	0.023*	s-Tg1	0.13
Gender	0.127	sup-Tg1	0.287
Tumor largest dimension	0.153	sup-TgAb1	0.092*
Cervical lymph node dissection	0.111	s-Tg2	0.050*
Tumor lesion	0.288	sup-Tg2	0.039*
Multifocality	0.16	$\Delta s\text{-Tg}$	0.020*
BRAF <sup>V600E</sup> mutation	0.037*	$\Delta s\text{-Tg}/\Delta s\text{-TSH}$	0.001*
AJCC-T Stage	0.083*	$\Delta s\text{-Tg}/\Delta s\text{-TSH}<1.5$	<0.01*
AJCC-N Stage	0.392		

\* $P<0.05$ ,  $\Delta s\text{-Tg}$ : s-Tg1/s-Tg2,  $\Delta s\text{-TSH}$ : s-TSH1/ s-TSH2.

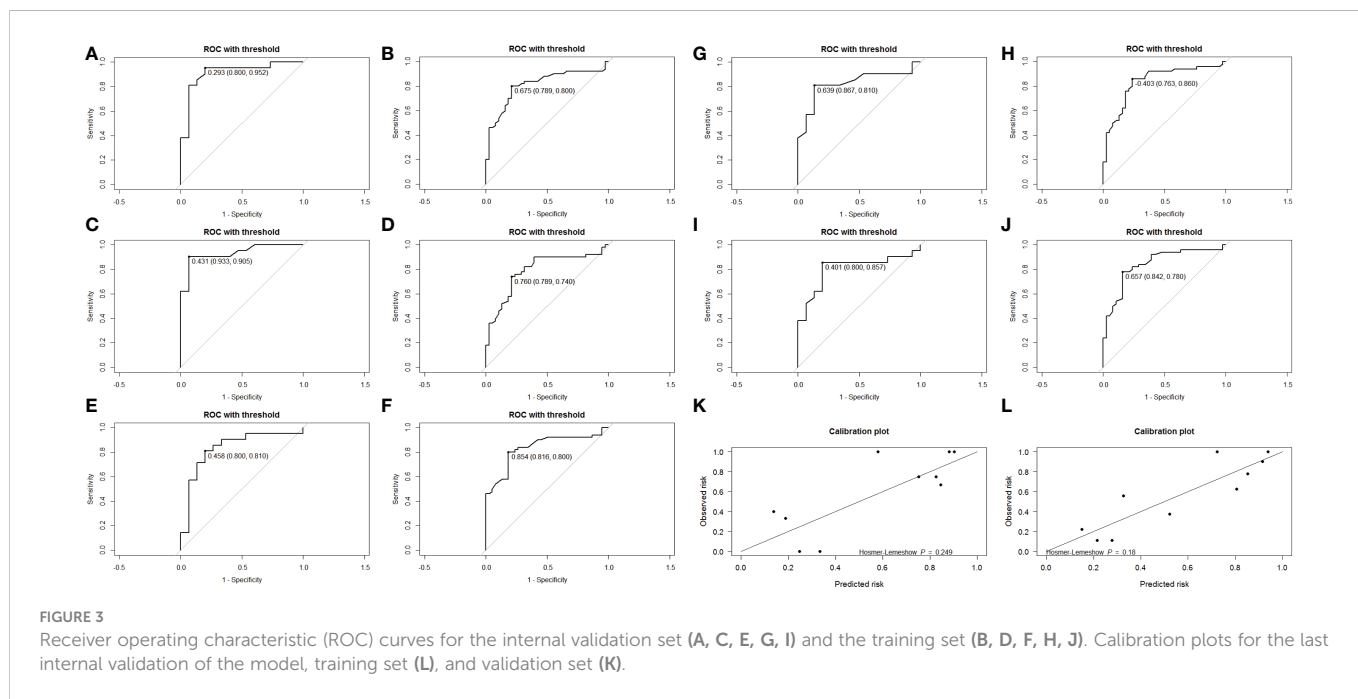


**FIGURE 3** Receiver operating characteristic (ROC) curves for the internal validation set (A, C, E, G, I) and the training set (B, D, F, H, J). Calibration plots for the last internal validation of the model, training set (K), and validation set (L).

**TABLE 3** Results of stepwise multivariate logistic regression on five random samples.

Independent risk factors	training set AUC	Internal validation set		
		AUC	Sensitivity	Specificity
$\Delta s\text{-Tg}/\Delta s\text{-TSH} < 1.50$ , Age upon diagnosis	0.810	0.913	0.952	0.800
	0.788	0.933	0.905	0.933
	0.834	0.832	0.810	0.800
	0.837	0.825	0.810	0.867
	0.842	0.805	0.857	0.800

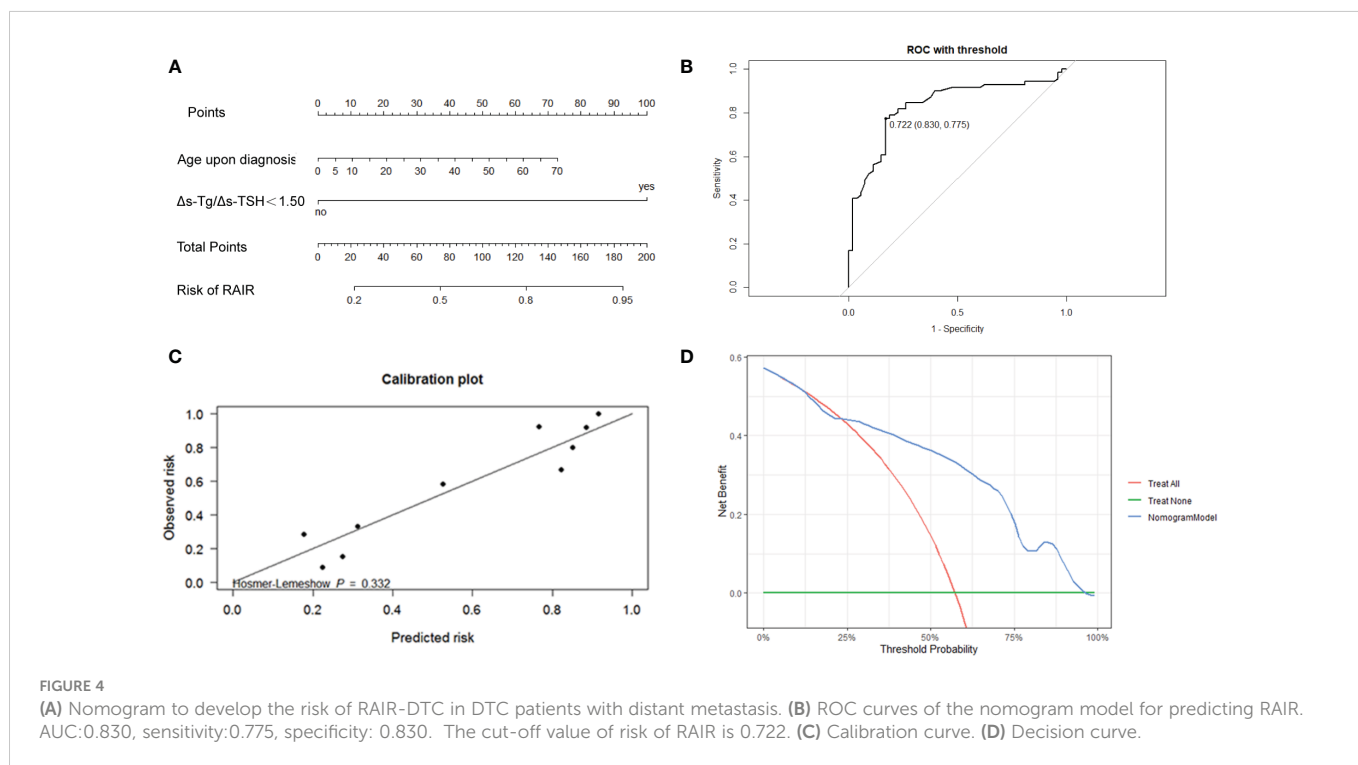


**FIGURE 4** (A) Nomogram to develop the risk of RAI-DTC in DTC patients with distant metastasis. (B) ROC curves of the nomogram model for predicting RAI. AUC:0.830, sensitivity:0.775, specificity: 0.830. The cut-off value of risk of RAI is 0.722. (C) Calibration curve. (D) Decision curve.

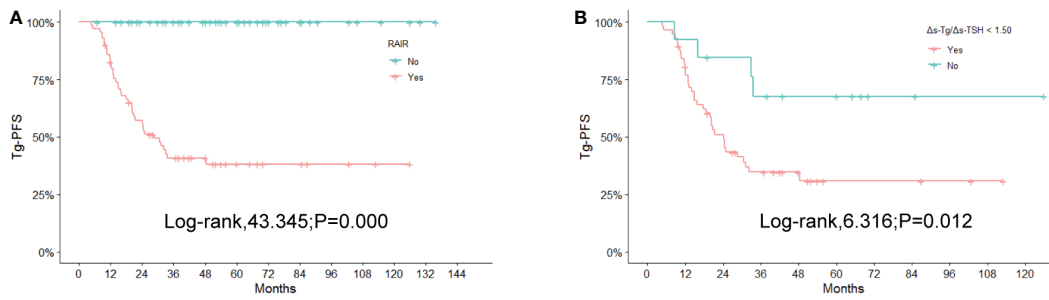


FIGURE 5 Kaplan-Meier curves for Tg-PFS (A) between non-RAIR and RAIR patients, (B) between RAIR patients with 1.50 of  $\Delta s\text{-Tg}/\Delta s\text{-TSH}$  as the cutoff value. RAIR, radioiodine refractory; Tg-PFS, thyroglobulin progression-free survival.

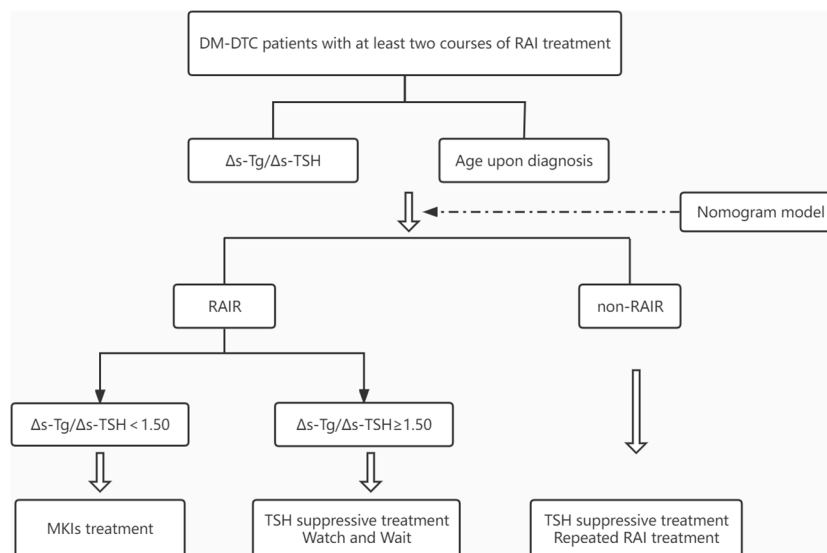


FIGURE 6 Flowchart for predicting RAIR and active surveillance of patients with DM-DTC. DM, distant metastases; DTC, differentiated thyroid cancer; TSH, thyroid stimulating hormone; MKIs, multi-kinase inhibitors.

$\Delta s\text{-TSH}$  was applied for the first time in this study to predict RAIR. Different from the previous Tg-relevant indicators, such a parameter not only associates Tg with TSH to make it standardized and comparable but also reflects the biochemical efficacy from RAI treatment longitudinally.

Age upon diagnosis was another important independent factor manifested in this study. Age has been associated with thyroid cancer staging, RAIR prediction, and risk of death. Age above 45 and over 55 years old were significant stratification factors in the TNM staging of thyroid cancer to differentiate the risk of death, in its 7th, and 8th editions, respectively (26, 27). Other researchers have reported a significant inverse correlation between RAI avidity and different age cut-offs, such as >45,  $\geq 46$ , or >55-years-old (13, 25, 28). A predictive value for OS of RAIR can be observed by using 45- and 75-years-old as cut-off, respectively (29). In a nomogram model to predict RAIR developed recently, an age cut-off of 48-years-old has also been integrated as an independent factor (18). Our finding revealed that age was also proved to be a significant predictor for RAIR as a continuous rather than a dichotomous variable in previous studies,

which presumably related to the wide range of age in the entire population in our research. Thus, it allows a specific personalized nomogram scoring in patients with different ages upon diagnosis.

Thus, unlike other scoring systems in identifying RAIR with either complex or high-cost index such as  $^{18}\text{F}\text{-FDG}\text{-PET}$  (18), we developed this nomogram model with promising predictive RAIR efficacy using two readily accessible factors described above. We believe it might be a user-friendly tool in routine clinical practice, particularly in China where recombinant human TSH (rhTSH) remains unavailable currently and thyroid hormone withdrawal is the only modality for TSH stimulation, which makes rhTSH aided-diagnostic RAI whole-body scan (DxWBS) for RAIR identification impossible. And due to its economic feasibility and practicability, our nomogram model might be an alternative for some other developing countries, where rhTSH cannot be affordable for most of the patients.

Interestingly, when we further evaluated the biochemical progression using a 20% change of Tg among all the generally so-called RAIR patients defined by ATA criteria, differing biochemical progression can be identified as rapidly or slowly progressive patients

with 1.50 as the  $\Delta s$ -Tg/ $\Delta s$ -TSH cut-off value. Patients with  $\Delta s$ -Tg/ $\Delta s$ -TSH <1.5 were apparently more progressive with a worse prognosis than those  $\geq 1.50$ . The biochemical response of Tg has been reported to reflect the general tumor burden and progression, and is associated with structural response or relapse assessed by RECIST criteria (23, 30–32). The classification of RAIR has long been argued with controversy, as the four or five clinical scenarios may have different underlying genetic backgrounds and clinical progressions but were dealt with solid arbitrary management (33, 34). With the index derived from our study, different clinical progression might be further identified, which may shed light on the personalized management in RAIR patients, and even be helpful to optimize the currently watchful waiting strategy, and to tailor the timing of initiating systemic therapy such as MKIs from a clinical perspective. A workable flowchart was also suggested in this study to guide the active surveillance among RAIR patients (Figure 6).

Although BRAF<sup>V600E</sup> mutation has been shown to be associated with RAIR (12, 35, 36), it was not manifested in the present study. We suppose the local genetic features reflected by the primary or regional tumor sites, or the heterogeneity between which might not thoroughly reflect the whole-body tumor genetic background, particularly the inaccessibility of distant metastasis due to ethic concern, while Tg, as a circulating marker, could comprehensively represent the overall biochemical tumor burden.

Our study is inevitably limited by its retrospective and single-center nature. Studies with larger sample sizes as well as multi-centers validation will be conducted subsequently.

In conclusion, we developed a convenient nomogram model integrating with Tg and age, which showed good predictive power for RAIR. By utilizing 1.50 as the cut-off value for  $\Delta s$ -Tg/ $\Delta s$ -TSH, the progression of RAIR may be further classified as a rapidly or slowly progressing group.

## Data availability statement

The raw data supporting the conclusions of this article will be made available by the authors, without undue reservation.

## References

- Sung H, Ferlay J, Siegel RL, Laversanne M, Soerjomataram I, Jemal A, et al. Global cancer statistics 2020: GLOBOCAN estimates of incidence and mortality worldwide for 36 cancers in 185 countries. *CA: Cancer J Clin* (2021) 71(3):209–49. doi: 10.3322/caac.21660
- Lim H, Devesa SS, Sosa JA, Check D, Kitahara CM. Trends in thyroid cancer incidence and mortality in the united states, 1974–2013. *Jama* (2017) 317(13):1338–48. doi: 10.1001/jama.2017.2719
- Sherman SI. Thyroid carcinoma. *Lancet (London England)* (2003) 361(9356):501–11. doi: 10.1016/s0140-6736(03)12488-9
- Wang LY, Palmer FL, Nixon IJ, Thomas D, Patel SG, Shaha AR, et al. Multi-organ distant metastases confer worse disease-specific survival in differentiated thyroid cancer. *Thyroid* (2014) 24(11):1594–9. doi: 10.1089/thy.2014.0173
- Mazzaferrri EL, Kloos RT. Clinical review 128: Current approaches to primary therapy for papillary and follicular thyroid cancer. *J Clin Endocrinol Metab* (2001) 86(4):1447–63. doi: 10.1210/jcem.86.4.7407
- Nixon IJ, Whitcher MM, Palmer FL, Tuttle RM, Shaha AR, Shah JP, et al. The impact of distant metastases at presentation on prognosis in patients with differentiated carcinoma of the thyroid gland. *Thyroid* (2012) 22(9):884–9. doi: 10.1089/thy.2011.0535
- Berdelou A, Lamartina L, Klain M, Leboulleux S, Schlumberger M. Treatment of refractory thyroid cancer. *Endocrine-related Cancer* (2018) 25(4):R209–23. doi: 10.1530/erc-17-0542
- Durante C, Haddy N, Baudin E, Leboulleux S, Hartl D, Travagli JP, et al. Long-term outcome of 444 patients with distant metastases from papillary and follicular thyroid carcinoma: benefits and limits of radioiodine therapy. *J Clin Endocrinol Metab* (2006) 91(8):2892–9. doi: 10.1210/jc.2005-2838
- Antonelli A, Ferri C, Ferrari SM, Sebastiani M, Colaci M, Ruffilli I, et al. New targeted molecular therapies for dedifferentiated thyroid cancer. *J Oncol* (2010) 2010:921682. doi: 10.1155/2010/921682
- Haugen BR, Alexander EK, Bible KC, Doherty GM, Mandel SJ, Nikiforov YE, et al. American Thyroid association management guidelines for adult patients with thyroid nodules and differentiated thyroid cancer: The American thyroid association guidelines task force on thyroid nodules and differentiated thyroid cancer. *Thyroid* (2015) 26(1):1–133. doi: 10.1089/thy.2015.0020
- Mu ZZ, Zhang X, Lin YS. Identification of radioactive iodine refractory differentiated thyroid cancer. *Chonnam Med J* (2019) 55(3):127–35. doi: 10.4068/cmj.2019.55.3.127

## Author contributions

JL and YL conceived and designed the study. CM and JS were the major contributors in performing the analysis, writing the manuscript, and preparing the figures and tables with support of WL. CM, JS, ZM, and YS collected samples and clinical parameters. JL and YL participated in the study design and edited the manuscript. All authors contributed to the article and approved the submitted version.

## Funding

This work was supported by the Project on National High Level Hospital Clinical Research Funding (No. 2022-PUMCH-B-072) and CAMS Innovation Fund for Medical Sciences (CIFMS) (No. 2020-I2M-2-003).

## Conflict of interest

The authors declare that the research was conducted in the absence of any commercial or financial relationships that could be construed as a potential conflict of interest.

## Publisher's note

All claims expressed in this article are solely those of the authors and do not necessarily represent those of their affiliated organizations, or those of the publisher, the editors and the reviewers. Any product that may be evaluated in this article, or claim that may be made by its manufacturer, is not guaranteed or endorsed by the publisher.

## Supplementary material

The Supplementary Material for this article can be found online at: <https://www.frontiersin.org/articles/10.3389/fendo.2023.1109439/full#supplementary-material>

12. Luo Y, Jiang H, Xu W, Wang X, Ma B, Liao T, et al. Clinical, pathological, and molecular characteristics correlating to the occurrence of radioiodine refractory differentiated thyroid carcinoma: A systematic review and meta-analysis. *Front Oncol* (2020) 10:549882. doi: 10.3389/fonc.2020.549882
13. Kersting D, Seifert R, Kessler L, Herrmann K, Theurer S, Brandenburg T, et al. Predictive factors for RAI-refractory disease and short overall survival in PDTC. *Cancers* (2021) 13(7):1728. doi: 10.3390/cancers13071728
14. Liu J, Liu R, Shen X, Zhu G, Li B, Xing M. The genetic duet of BRAF V600E and TERT promoter mutations robustly predicts loss of radioiodine avidity in recurrent papillary thyroid cancer. *J Nucl Med* (2020) 61(2):177–82. doi: 10.2967/jnumed.119.227652
15. Mao Q, Xia W, Dong G, Chen S, Wang A, Jin G, et al. A nomogram to predict the survival of stage IIIA-N2 non-small cell lung cancer after surgery. *J Thorac Cardiovasc Surg* (2018) 155(4):1784–92. doi: 10.1016/j.jtcvs.2017.11.098
16. Lv J, Liu YY, Jia YT, He JL, Dai GY, Guo P, et al. A nomogram model for predicting prognosis of obstructive colorectal cancer. *World J Surg Oncol* (2021) 19(1):337. doi: 10.1186/s12957-021-02445-6
17. Li G, Lei J, Song L, Jiang K, Wei T, Li Z, et al. Radioiodine refractoriness score: A multivariable prediction model for postoperative radioiodine-refractory differentiated thyroid carcinomas. *Cancer Med* (2018) 7(11):5448–56. doi: 10.1002/cam4.1794
18. Liu Y, Wang Y, Zhang W. Scoring system and a simple nomogram for predicting radioiodine refractory differentiated thyroid cancer: a retrospective study. *EJNMMI Res* (2022) 12(1):45. doi: 10.1186/s13550-022-00917-8
19. Yang X, Liang J, Li T, Zhao T, Lin Y. Preablative stimulated thyroglobulin correlates to new therapy response system in differentiated thyroid cancer. *J Clin Endocrinol Metab* (2016) 101(3):1307–13. doi: 10.1210/jc.2015-4016
20. Yang X, Liang J, Li TJ, Yang K, Liang DQ, Yu Z, et al. Postoperative stimulated thyroglobulin level and recurrence risk stratification in differentiated thyroid cancer. *Chin Med J* (2015) 128(8):1058–64. doi: 10.4103/0366-6999.155086
21. Tian T, Xu Y, Zhang X, Liu B. Prognostic implications of preablation stimulated tg: A retrospective analysis of 2500 thyroid cancer patients. *J Clin Endocrinol Metab* (2021) 106(11):e4688–97. doi: 10.1210/clinem/dgab445
22. Zhao T, Liang J, Li T, Guo Z, Vinjamuri S, Lin Y. Value of serial preablative thyroglobulin measurements: can we address the impact of thyroid remnants? *Nucl Med Commun* (2016) 37(6):632–9. doi: 10.1097/mnm.0000000000000485
23. Mu ZZ, Zhang YQ, Sun D, Lu T, Lin YS. Effect of BRAF(V600E) and TERT promoter mutations on thyroglobulin response in patients with distant-metastatic differentiated thyroid cancer. *Endocrine Pract* (2022) 28(3):265–70. doi: 10.1016/j.eprac.2021.12.005
24. Matthews TJ, Chua E, Gargya A, Clark J, Gao K, Elliott M. Elevated serum thyroglobulin levels at the time of ablative radioactive iodine therapy indicate a worse prognosis in thyroid cancer: An Australian retrospective cohort study. *J Laryngol Otol* (2016) 130(Suppl 4):S50–3. doi: 10.1017/s0022215116008331
25. Wang C, Zhang X, Li H, Li X, Lin Y. Quantitative thyroglobulin response to radioactive iodine treatment in predicting radioactive iodine-refractory thyroid cancer with pulmonary metastasis. *PLoS One* (2017) 12(7):e0179664. doi: 10.1371/journal.pone.0179664
26. Onitilo AA, Engel JM, Lundgren CI, Hall P, Thalib L, Doi SA. Simplifying the TNM system for clinical use in differentiated thyroid cancer. *J Clin Oncol* (2009) 27(11):1872–8. doi: 10.1200/jco.2008.20.2382
27. Kim M, Kim YN, Kim WG, Park S, Kwon H, Jeon MJ, et al. Optimal cut-off age in the TNM staging system of differentiated thyroid cancer: is 55 years better than 45 years? *Clin Endocrinol* (2017) 86(3):438–43. doi: 10.1111/cen.13254
28. Shobab L, Gomes-Lima C, Zeymo A, Feldman R, Jonklaas J, Wartofsky L, et al. Clinical, pathological, and molecular profiling of radioactive iodine refractory differentiated thyroid cancer. *Thyroid* (2019) 29(9):1262–8. doi: 10.1089/thy.2019.0075
29. Saie C, Wassermann J, Mathy E, Chereau N, Leenhardt L, Tezenas du Montcel S, et al. Impact of age on survival in radioiodine refractory differentiated thyroid cancer patients. *Eur J Endocrinol* (2021) 184(5):667–76. doi: 10.1530/eje-20-1073
30. Bachelot A, Cailleux AF, Klain M, Baudin E, Ricard M, Bellon N, et al. Relationship between tumor burden and serum thyroglobulin level in patients with papillary and follicular thyroid carcinoma. *Thyroid* (2002) 12(8):707–11. doi: 10.1089/105072502760258686
31. Ciappuccini R, Hardouin J, Heutte N, Vaur D, Quak E, Rame JP, et al. Stimulated thyroglobulin level at ablation in differentiated thyroid cancer: the impact of treatment preparation modalities and tumor burden. *Eur J Endocrinol* (2014) 171(2):247–52. doi: 10.1530/eje-14-0192
32. Spaas M, Decallonne B, Laenen A, Billen J, Nuyts S. Prognostic value of stimulated thyroglobulin levels at the time of radioiodine administration in differentiated thyroid cancer. *Eur Thyroid J* (2018) 7(4):211–7. doi: 10.1159/000489849
33. Tuttle RM, Ahuja S, Avram AM, Bernet VJ, Bourguet P, Daniels GH, et al. Controversies, consensus, and collaboration in the use of (131)I therapy in differentiated thyroid cancer: A joint statement from the American thyroid association, the European association of nuclear medicine, the society of nuclear medicine and molecular imaging, and the European thyroid association. *Thyroid* (2019) 29(4):461–70. doi: 10.1089/thy.2018.0597
34. Van Nostrand D. Radioiodine refractory differentiated thyroid cancer: Time to update the classifications. *Thyroid* (2018) 28(9):1083–93. doi: 10.1089/thy.2018.0048
35. Yang K, Wang H, Liang Z, Liang J, Li F, Lin Y. BRAFV600E mutation associated with non-radioiodine-avid status in distant metastatic papillary thyroid carcinoma. *Clin Nucl Med* (2014) 39(8):675–9. doi: 10.1097/rlu.0000000000000498
36. Tchekmedyian V, Dunn L, Sherman E, Baxi SS, Grewal RK, Larson SM, et al. Enhancing radioiodine incorporation in BRAF-mutant, radioiodine-refractory thyroid cancers with vemurafenib and the anti-ErbB3 monoclonal antibody CDX-3379: Results of a pilot clinical trial. *Thyroid* (2022) 32(3):273–82. doi: 10.1089/thy.2021.0